ANALYSIS OF NO FORMATION IN COUNTER-FLOW PREMIXED HYDROGEN-AIR FLAME

Tianfang Xie and Peiyong Wang
Department of Aeronautics, Xiamen University, Xiamen, China
E-mail: tianfang.xie@stu.xmu.edu.cn; peiyong.wang@xmu.edu.cn

ICETI 2012-J1157_SCI
No. 13-CSME-71, E.I.C. Accession 3529

ABSTRACT

Though hydrogen fuel reduces the carbon dioxide emission, it still produces NO_x. However, gaps exist in the fundamental understanding of hydrogen-air combustion and the NO emission; most previous research has focused on the flames burning with mixture such as H_2 mixed with CH4, rather than pure H_2 flame. Here, a computational study is presented to investigate the stretch effect on NO formation in counter-flow premixed hydrogen-air flame. The simulation of premixed hydrogen flame was performed with OPPDIF code and UCSD chemical mechanism. Result indicates that the NO formation is affected by three factors: radical concentration, flame temperature, and residence time of reactants. The flame temperature, the reaction rate of NO, and the NO emission index all decrease when the stretch rate increases. Moreover, the formation of NO through thermal mechanism, NNH mechanism, and N_2O mechanism is discussed, as well as the percentage of their contribution.

Keywords: premixed flame; NO emission; counter-flow flame; stretch effect.

L'ANALYSE DE LA FORMATION DU NO DANS LA FLAMME Á CONTRE-COURANT PRÉMÉLANGÉ PAR L'HYDROGÈNE ET L'AIR

RÉSUMÉ

Bien que le combustible hydrogène puisse réduire l'émission du dioxyde de carbone, il produit des oxydes d'azote. Ni l'étude du mélange de l'hydrogène et l'air, ni l'émission du NO n'avaient été réalisée avant. La plupart des études se sont concentrées sur la combustion du mélange de l'hydrogène et d'un autre gaz. L'exemple classique est celui de l'hydrogène et le méthane. Ce travail analyse l'influence de l'allongement de flamme à contre-courant prémélangé par l'hydrogène et l'air sur l'émission du monoxyde d'azote par une méthode numérique. La modélisation de la flamme prémélangée est réalisée par l'application des codes de calcul OPPDIF en comprenant le mécanisme chimique UCSD. Nos résultats montrent que trois facteurs sont déterminants pour la formation du NO : la concentration des radicaux libres, la température de flamme et le temps de séjour. Plus l'allongement de flamme est grand, plus la température de flamme, la vitesse de formation et l'indice d'émission du NO sont petits. La formation du NO des différents mécanismes et leurs pourcentages de contribution sont discutés.

Mots-clés : la flamme prémélangée ; l'influence de l'allongement de flamme.

1. INTRODUCTION

Due to the global environmental devastation, the concern about the fuel shortage and air pollution control has been increased. Over the last 30 years, all industrialized countries and many developing countries have introduced increasingly stringent legislation restricting the level of pollutant emission. Reducing exhaust emissions has become a major topic of the combustion research. Engineers and scientists are trying to promote the use of clean energy and renewable energy to replace the fossil fuel. For example, natural gas became one of the world's most abundant sources of primary energy, and has been in use as a transportation fuel [1]. Although hydrogen has considerably low density and its efficient production and storage is difficult currently, it has the advantages of large combustion heat release per unit mass and little harmful emission during inflammation; there is no CO, SO_x, PAH, soot, and unburned hydrocarbon emission from the hydrogen fuel combustion, it also does not produce the greenhouse gas CO_2. Besides, hydrogen has a wide ignition limits of mixtures with air, from $\lambda = 0.14$ to $\lambda = 10$ homogeneous [2]. So more fundamental study of the hydrogen-air premixed flame is needed to understand its burning characteristics and chemical kinetics.

The only pollutant from hydrogen combustion is NO_x, so the reduction of NO_x emission is much more important than that of combustion with conventional fuels. Therefore, the $H_2/O_2/N_2$ kinetics is important for accurate prediction of NO_x formation. And the study of combustion characteristics and NO_x behavior of hydrogen fuel combustion is necessary before extensive usage of hydrogen fuel.

The counterflow flame has been used in many studies to investigate the reaction kinetics and species transport model under the influence of aerodynamic stretch, which led to a better understanding of the structure and propagation of laminar premixed flames [3]. It also has been used frequently in combustion NO_x emission studies. Skottene and Rian [4] studied NO_x formation numerically in the premixed hydrogen flames and compared them with the experimental data. Their results showed that the formation of NO through NNH radicals is important in the hydrogen-air flames; the flame temperature and the radical production have a strong influence on the NO_x predictions. Frassoldati and Faravelli [5] have investigated the NO_x formation and nitrogen chemistry in the hydrogen flame with a large set of experimental data. Their investigation showed that two main reaction paths of NO_x formation are relevant in H_2 combustion: thermal NO and the N_2O mechanism; the NNH mechanism is important at low temperatures too. Guo et al. [6] numerically investigated the effect of hydrogen addition on the extinction limits and the characteristics of NO_x emission of the ultra-lean counterflow CH_4/air premixed flame. They found that the addition of hydrogen can significantly increase the flammable region and extend the flammability limit of stretched flame to a lower equivalence ratio. However, none of them have investigated the NO formation in counter-flow premixed hydrogen-air combustion. In this paper, the stretch effect on NO generation in counter-flow premixed hydrogen-air flames is systematically investigated for the first time.

2. NUMERICAL MODEL

Simulations of premixed hydrogen flames are performed with the OPPDIF code [7] of the CHEMKIN package [8]. The OPPDIF code is written in FORTRAN, and used for computing combustion in a counterflow configuration. The transport model includes multi-component gas diffusion and the thermal diffusion of light species such as H_2 and H. The OPPDIF code has been widely used in the premixed flame simulation; numerous successful research has validated the accuracy of the code [9].

Small adaptive grid adjustment parameters are adopted in the simulation. The values of GRAD and CURV are all 0.03 to ensure that there are sufficient nodes and simulation results are independent of the number of nodes. Strict convergence criteria is also introduced to reduce the computational truncation error, and the RTOL is 1.E-10, ATOL is 1.E-12, ATIM is 1.E-12 and RTIM is 1.E-10, respectively [10]. Because the impact of radiation on the hydrogen flame temperature is considerably small, the simulation does not include

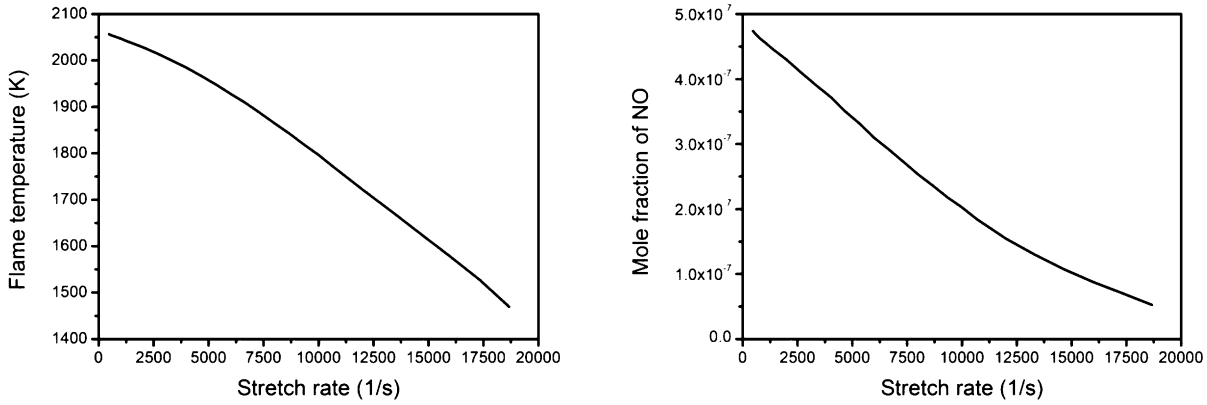

Fig. 1. Flame temperature and peak NO concentration variation with stretch rate.

the radiation model. The temperature of both fresh mixture streams is set as 298 K. The global stretch rate is defined as

$$k = \frac{4V}{L} \tag{1}$$

where L is the distance between the two nozzles, which is set as 3 cm, and V is the velocity out of the nozzles [11].

The reaction kinetics is modeled by the UCSD mechanism from the University of California at San Diego [12]. Li et al. [10] proved the accuracy of the kinetic mechanism for NO_x emission; compared with experiment data, the difference for flame temperature and NO_x emission are within 30 K and 2 ppm respectively, which are within the experiment uncertainty.

It is well known that NO can be formed through the thermal route, the N_2O intermediate route, NNH route, and the prompt route. The hydrogen combustion does not contain hydrocarbon radical; therefore, the prompt route does not exist. Thus the important routes for NO formation in hydrogen flames are the thermal route, the N_2O route, and the NNH route. The thermal NO mechanism consists of three reactions: $N_2 + O = N + NO$; $N + O_2 = NO + O$; and $N + OH = NO + H$; because the initiation reaction has high activation energy, the thermal route is strongly dependent on flame temperature. The N_2O intermediate route is initiated by these reactions: $N_2O + M = N_2 + O + M$; $N_2O + H = N_2 + OH$; $N_2O + O = N_2 + O_2$; and $N_2O + OH = N_2 + HO_2$; and for this route, the formation of NO is promoted at high pressure due to the presence of a third body. The essential reactions of the NNH route are: $N_2 + H = NNH$; $NNH + O = NO + NH$; it can also be initiated by the reactions of molecular nitrogen with other hydrocarbon-free radicals, such as H, OH, and H_2. The NNH pathway appears to be important at flame fronts and other areas where relatively high concentrations of H and O radicals are present.

3. RESULTS AND DISCUSSIONS

3.1. Stretch Effect on NO Concentration

Since the objective of this paper is to study the effect of stretch rate on NO formation in counter-flow premixed hydrogen-air flame, a constant equivalence ratio of 2 is used for all the flames.

Figure 1 shows the peak temperature and the peak NO concentration (at the symmetric plane) variation with stretch rate. It is observed that the flame temperature and the peak NO mole fraction decreased with stretch rate.

The Lewis number of the flame is evaluated based on the mass diffusivity of O_2 in the mixture since O_2 is the deficient reactant. For a premixture with *Le* less than one, when the stretch rate increases, the

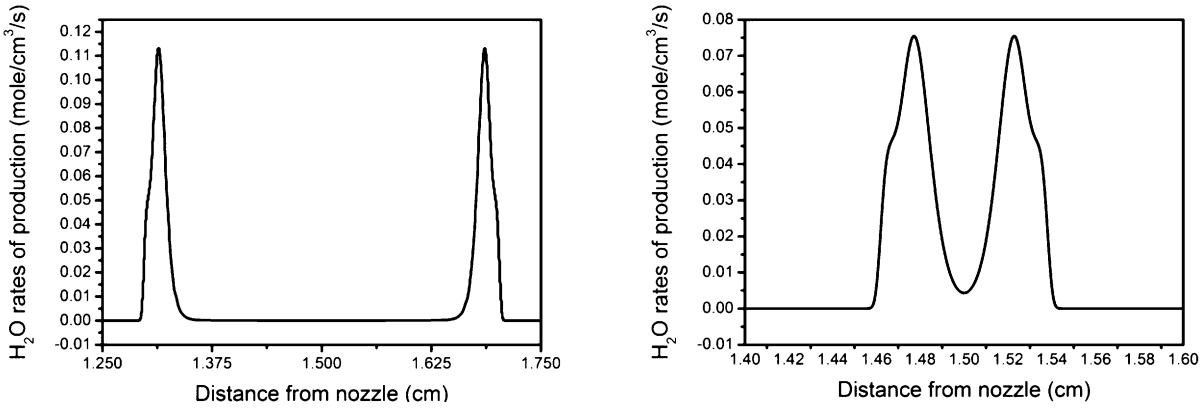

Fig. 2. H_2O production rates for two different stretch rates (Left: 4000 s^{-1}, Right: 17333.33 s^{-1}).

flame temperature increases, and for a premixture with *Le* more than one, increasing the stretch rate will decrease the flame temperature continuously until extinction [11]. In this simulation, the calculated *Le* is 1.74. Therefore, the flame temperature will decrease when the stretch rate increases.

The H_2O production rates with stretch rates 4000 and 17333.33 s^{-1} are given in Fig. 2. It can be clearly observed that the H_2O production rate is symmetrical about the stagnation plane. When the stretch rate is low, there is no H_2O generated in the stagnation region, which means the O_2 sufficiently react with H_2 before it reaches the stagnation plane. When the stretch rate increases to a very large value, the H_2O is even generated in the stagnation plane which means the reaction between H_2 and O_2 does not proceed completely. When the stretch rate gradually increases, the exit velocity of the premixed stream is growing; it pushes the flames get closer and closer to the stagnation plane. The residence time of reactants in the flame zone has also become shorter. When this residence time is less than the chemical reaction time, the chemical reactions are incomplete. The incomplete reaction also causes the temperature decrease. When the exit velocity of the fresh mixture reaches a critical value, the flame will be extinguished at the center of the burner. In addition, the NO emission is also a sensitive function to the flame temperature, and can be affected by the radical H and O concentrations.

The residence time is proportional to the reciprocal of stretch rate as in [13]. The NO generation is proportional to the residence time in the flame zone including combustion zone and post flame zone, the relationship between the NO emission and the residence time of reactants in the flame zone will be verified. The residence time has been defined as the time of reactant traveling from the peak O concentration point. Figure 3a shows the O mole fraction distribution for flames with different stretch rates. It illustrates that as the stretch rate increases, the average O concentration in the post flame zone gradually increases and the peak O concentration decreases; same trends are observed for OH, H, N radicals. The free radicals such as H, O and OH are extremely active due to the presence of unpaired electrons and are short-lived during combustion. The chain branching and chain propagating reactions initiated by free radicals play the most important role in chemical reaction [14]. The relationship between the NO mole fraction and the residence time is shown in Fig. 3b. It can be seen that the NO concentration with different stretch rates can be divided into two parts: one part has a linear relationship with the residence time and another almost flat part. The linear region represents the combustion zone and most of the post flame zone, NO mass diffusion is much less than convection and production terms in this region and can be ignored, thus the slope of the NO mole fraction curve is proportional to the NO formation rate. As shown in Fig. 3b, with the increasing of stretch rate, the slope of the NO mole fraction curve decreases, and the maximum value of the linear region is also decreasing. The flat part represents a very tiny region around the stagnation plane, the volume of this region

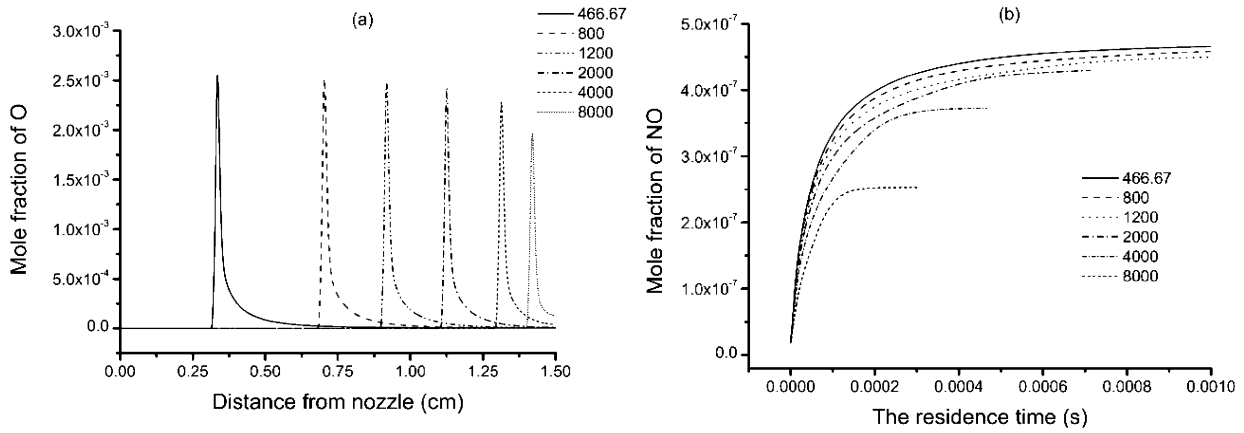

Fig. 3. O mole fraction distribution of different stretch rates (466.67, 800, 1200, 2000, 4000, and 8000 s^{-1}, respectively) (a). NO mole fraction variation with residence time for different stretch rates (b).

Table 1. Variables at the stagnation plane.

Stretch rate (s^{-1})	800	8000
Temperature(K)	2050.55	1864.58
Mole fraction of NH	2.71E-10	4.03E-10
Mole fraction of O	2.55E-06	0.00013
NO rates of production (mole/cm^3-s)	7.25E-11	4.34E-09

is very small, and so is the NO production. At the same time, the axial velocity is tiny, so the residence time appears high; with the large variation of residence time and very tiny NO production, the flat characteristics of the curves are observed.

3.2. Stretch Effect on NO Production

Figure 4 shows the NO formation data with different stretch rates. The biggest difference among these four figures is that when the stretch rate is low, the NO production rate near the axis of symmetry approaches 0, but when the stretch is very high, such as 8000 s^{-1}, the NO production rate near the axis of symmetry was significantly increased. To explain this phenomenon, one reaction $N + OH = NO + H$ is chosen for detailed study because its curves vary obviously, and the related variables at the stagnation plane with stretch rate 800 s^{-1} and 8000 s^{-1} are listed in Table 1.

For the reaction $NH + O = NO + H$, according to the Arrhenius reaction rate we have

$$\dot{\omega}_{NO} = AT^{b}[NH][O]\exp\left(-\frac{E_a}{RT}\right) \tag{2}$$

where the parameter b and the activation energy E_a both are zero. The O mole fraction with stretch rate 8000 s^{-1} is much larger than that with stretch rate 800 s^{-1}. The reactions of H_2 and O_2 proceed completely before reaching the stagnation plane with stretch rate 800 s^{-1}, the stagnation region is the post flame region with low radical concentration; with stretch rate 8000 s^{-1}, the reactions of H_2 and O_2 are still going on at the stagnation plane, and the stagnation region is the combustion zone with very high radical concentration. Therefore the NO production rate in the stagnation plane is much higher in the case with stretch rate 8000 s^{-1}.

In Fig. 4, it is observed that the reaction $HNO + M = H + NO + M$ has a negative value for NO production; the reaction is going in the reverse direction and consumes NO significantly. In addition, the reaction

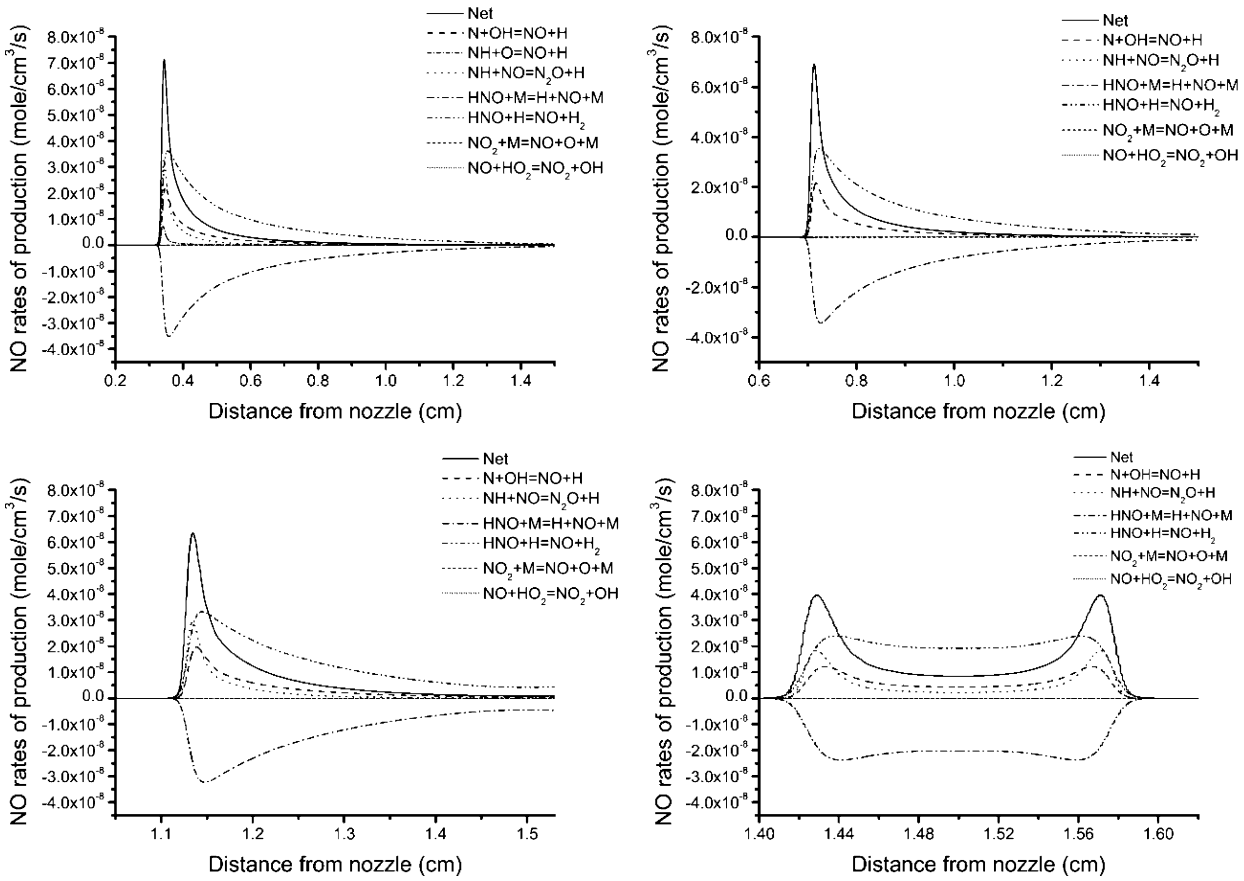

Fig. 4. NO formation data with different stretch rates (466.67, 800, 2000, and 8000 s^{-1}, respectively).

$NO_2 + M = NO + O + M$ and reaction $NO + HO_2 = NO_2 + OH$ are the mechanism of the transformation between NO and NO_2. Only at low temperature could NO be transformed to NO_2 significantly, but this is not the situation here and the transformation rate is very little.

In current simulations, the N_2O route contributes very little to the NO production because the NO formation is promoted at high pressure with the N_2O route due to the presence of a third body in reaction $N_2 + O + M = N_2O + M$, and the current simulations are under one atmospheric pressure.

As the flame temperatures for these four stretch rates are 2057, 2051, 2029, and 1865 K, respectively, the NO formation mechanism of all four flames contains thermal type and NNH type. Figure 5 shows the total NO production (integration over axial distance) by thermal mechanism, NNH mechanism, and the full mechanism. For the flame with a relatively high temperature 2057 K (466.66 s^{-1}), the thermal-type mechanism contributes 52.1% of the total NO production. It only contributes 43.4% of the total NO production with 8000 s^{-1}, 1865 K. The NNH pathway reactions occur mainly in the combustion zone with relatively high concentrations of H and O radicals. We can calculate from Fig. 5, that the NNH type reactions $NH + O = NO + H$, $NH + NO = N_2O + H$, and $HNO + H = NO + H_2$ contribute 47.7% of total NO formation with 466.66 s^{-1}, and 56.2% of total NO formation with 8000 s^{-1}, respectively.

The total NO production rate in Fig. 5 is affected by the NO production rate and the production volume. For the thermal mechanism, the NO production rate can be written as

$$\dot{\omega}_{NO} = 2k_1[O][N_2] \tag{3}$$

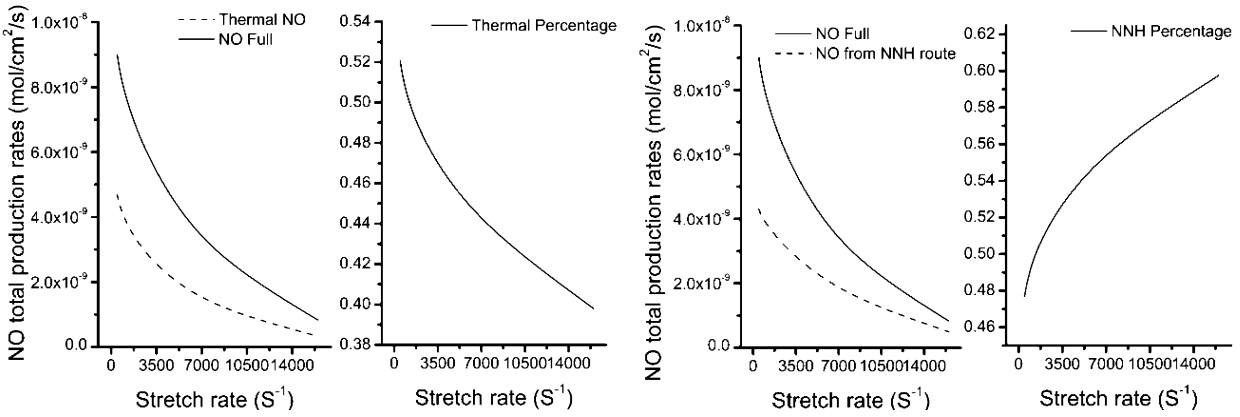

Fig. 5. Contributions of thermal route and NNH route to the total NO production rates with different stretch rates.

where k_1 is the rate coefficient $1.8 \times 10^{-10} \exp(-38400/T)$ cm^3 mol^{-1}s^{-1} [15]. The NO production rate via the NNH mechanism at 1 atm is

$$\dot{\omega}_{\mathrm{NO}} = 2k_2k_p\ [\mathrm{N_2}][\mathrm{O}]\mathrm{X_H} \tag{4}$$

where k_p is the equilibrium constant of reaction $\mathrm{N_2 + H = NNH}$ in partial pressures, X_H is the H mole fraction [16], and k_2k_p equals $2.3 \times 10^{-15} \exp(-2760/T)$ cm^{3}mol^{-1}s^{-1}. The coefficient k_1 has a large activation temperature; which causes the thermal type NO production rate decreases very rapidly with stretch rate. The effective rate k_2k_p is relatively insensitive to temperature because of lower activation temperature, thus the NO production rate with NNH type is proportional to the H and O concentrations. As mentioned before, the peak O and H concentration are all decreasing with stretch rate, which makes the reduction of NO production rate with NNH type. The thermal type NO production rate decreases with temperature relatively faster and caused the NNH type NO production occupied a larger percentage.

The production volume of NO includes the combustion zone and the post flame zone. The thermal type NO production appears not only in the combustion zone but also the post flame zone and the NNH type NO is mainly generated in the combustion zone. The combustion zone and post flame zone all decrease as the stretch rate increases, thus the thermal type NO production will be more affected; which also makes the NNH type NO production shows a larger percentage.

3.3. Stretch Effect on NO Emission Index

The global NO characteristics of hydrogen-air flames with different stretch rates can be compared by plotting the NO emission index versus global stretch rate. The NO emission index (EINO) is defined as

$$\mathrm{EINO} = \frac{\int_0^L M_{\mathrm{NO}} \dot{\omega}_{\mathrm{NO}} dx}{-\int_0^L M_{\mathrm{fuel}} \dot{\omega}_{\mathrm{fuel}} dx} \tag{5}$$

where M represents the molecular weight, $\dot{\omega}$ is the net production/consumption rate, L is the distance between the nozzles, and x is the axial coordinate [17]. The emission index is a global parameter that has been commonly used to characterize NO emission from different flames. Since the fuel is pure H_2 in this simulation, the above equation is written as

$$\mathrm{EINO} = \frac{\int_0^L M_{\mathrm{NO}} \dot{\omega}_{\mathrm{NO}} dx}{-\int_0^L M_{\mathrm{H_2}} \dot{\omega}_{\mathrm{H_2}} dx} \tag{6}$$

The H_2 consumption rate and the NO production rate with different stretch rates are shown in Figs. 6a and 6b respectively. As shown in Fig. 6c, the integration terms of NO production and H_2 consumption all

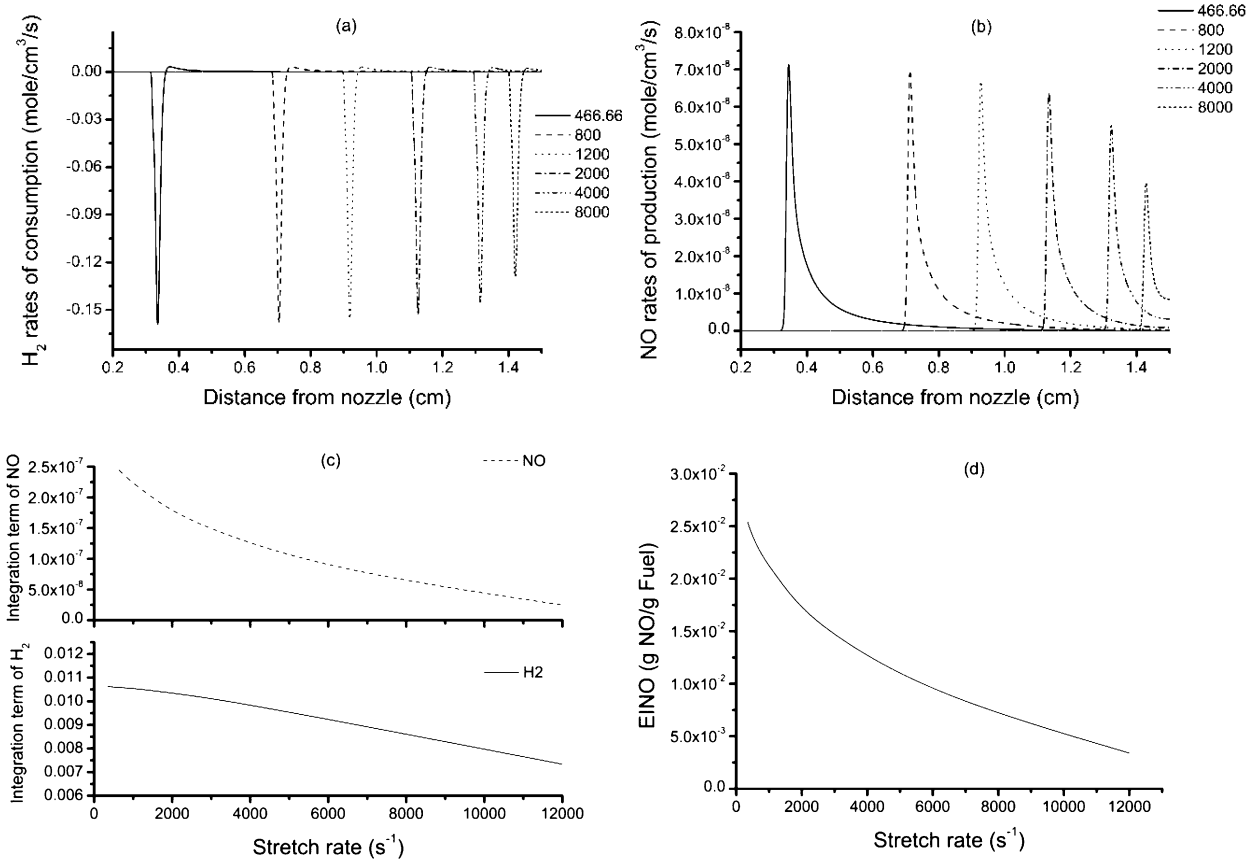

Fig. 6. The H_2 rates of consumption (a); the NO rates of production (b); the integration terms of NO and H_2 (c); the NO emission index (d).

decreases with stretch rate. As mentioned before, with increasing stretch rate, the integral terms of NO production decreases due to the lower temperature and lower NO reaction volume (combustion zone plus post flame zone). The reduction of the integration term of H_2 consumption is caused by the reduction of reaction rate due to lower temperature and the combustion zone thickness as stretch rate increases. The production volume of NO including the combustion zone and post flame zone, it decreases very fast with stretch rate as the flame is pushed to the stagnation plane, while the combustion zone alone (H_2 consumption volume) decreases slowly with stretch rate. The volume effect combining with the flame temperature effect on reaction rate causes the NO total production decrease faster than that of hydrogen consumption; the NO emission index (EINO) shows a downward trend in Fig. 6d.

4. CONCLUSIONS

A computational study of the stretch effect on NO formation in counter-flow premixed hydrogen-air flame is presented. An equivalence ratio of 2 is used for all the flames. The focus of the study is the effect of stretch rate on flame temperature and NO concentration as well as the stretch effect on NO production and NO emission index. Important observations are as follows:

1. The Lewis number of this flame is 1.74, therefore, the flame temperature decreases with stretch rate because of preferential diffusion effect and incomplete reactions. And the peak NO mole fraction decreases with the stretch rate owing to the lower temperature and shorter residence time of reactants.

2. For the current simulations, the thermal route and NNH route are the dominant NO production mechanism. Their relative contribution depends on stretch rate. At low stretch rate, the temperature is high and thermal mechanism contributes more to the total NO production and vice versa for the high stretch rate situation.

3. The total NO production decreases with stretch rate because of decreasing temperature and reaction volume. The H_2 consumption deceases with stretch rate due to the flame thickness reduction and lower flame temperature. The total NO production decreases with stretch rate relatively faster and caused the NO emission index decrease with stretch rate.

REFERENCES

1. Boretti, A.A., "Numerical evaluation of the performance of a compression ignition CNG engine for heavy duty trucks with an optimum speed power turbine", *International Journal of Engineering and Technology Innovation*, Vol. 1, No. 1, pp. 12–26, 2011.
2. Boretti, A.A., "Simulations of multi combustion modes hydrogen engines for heavy duty trucks", *International Journal of Engineering and Technology Innovation,* Vol. 2, No. 1, pp. 13–30, 2012.
3. Law, C. and Sung, C., "Structure, aerodynamics, and geometry of premixed flamelets", *Progress in Energy and Combustion Science*, Vol. 26, pp. 459–505, 2000.
4. Skottene, M. and Rian, K.E., "A study of NO_x formation in hydrogen flames", *International Journal of Hydrogen Energy*, Vol. 32, pp. 3572–3585, 2007.
5. Frassoldati, A., Faravelli, T. and Ranzi, E., "A wide range modeling study of NO_x formation and nitrogen chemistry in hydrogen combustion", *International Journal of Hydrogen Energy*, Vol. 31, pp. 2310–2328, 2006.
6. Guo, H., Smallwood G.J., Liu, F., Ju, Y. and Gülder, Ö.L., "The effect of hydrogen addition on flammability limit and NO_x emission in ultra-lean counterflow CH_4/air premixed flames", In *Proceedings of the Combustion Institute*, Vol. 30, pp. 303–311, 2005.
7. Lutz, A.E., Kee, R.J., Grcar, J.F. and Rupley, F.M., "OPPDIF: A Fortran program for computing opposed-flow diffusion flames", Sandia National Laboratories Report SAND96-8243, 1997.
8. Kee, R.J., Rupley, F., Miller, J., Coltrin, M., Grcar, J., Meeks, E., Moffat, H., Lutz, A., Dixon-Lewis, G., Smooke, M., Warnatz, J., Evans, G., Larson, R., Mitchell, R., Petzold, L., Reynolds, L., Caracotsios, M., Stewart, W., Glarborg, P., Wang, C. and Adigun, O., CHEMKIN Collection, Release 3.6, Reaction Design, Inc., San Diego, CA, 2000.
9. Hu, S., Wang, P. and Pitz, R.W., "A structural study of premixed tubular flames", In *Proceedings of the Combustion Institute*, Vol. 32, pp. 1133–1140, 2009.
10. Li, Q., Wang, P., Xing, F. and Zou, J., "Flame curvature effect on NO emission of the hydrogen diffusion flame", *Journal of Engineering Thermo-physics*, Vol. 32, pp. 1949–1952, 2011.
11. Wang, P., Wehrmeyer, J.A. and Pitz, R.W., "Stretch rate of tubular premixed flames", *Combustion and Flame*, Vol. 145, pp. 401–414, 2006.
12. Williams, F.A., Sandiego 20051201-CK.txt, NOXsandiego20041209.mechttp://mac.ucsd.edu/combustion/cermech
13. Kobayashi, H. and Kitano, M., "Flow fields and extinction of stretched cylindrical premixed flames", *Combustion Science and Technology*, Vol. 75, pp. 227–239, 1991.
14. Zheng, J., Zhang, Z., Huang, Z., Hu, E., Tang, C. and Wang, J., "Numerical study on combustion of diluted methanol-air premixed mixtures", *Chinese Science Bulletin*, Vol. 55, pp. 882–889, 2010.
15. Turns, S.R., "Understanding NO_x formation in nonpremixed flames: Experiments and modeling", *Progress in Energy and Combustion Science*, Vol. 21, pp. 361–385, 1995.
16. Hayhurst, A. and Hutchinson, E., "Evidence for a new way of producing NO via NNH in fuel-rich flames at atmospheric pressure", *Combustion and Flame*, Vol. 114, pp. 274–279, 1998.
17. Naha, S. and Aggarwal, S.K., "Fuel effects on NO_x emissions in partially premixed flames", *Combustion and Flame*, Vol. 139, pp. 90–105, 2004.